Meteoritics & Planetary Science 40, Nr 12, 1859–1877 (2005)
Abstract available online at http://meteoritics.org

A case study of impact-induced hydrothermal activity: The Haughton impact structure, Devon Island, Canadian High Arctic

Gordon R. OSINSKI[1†*], Pascal LEE[2], John PARNELL[3], John G. SPRAY[4], and Martin BARON[3]

[1]Lunar and Planetary Laboratory, University of Arizona, 1629 East University Boulevard, Tucson, Arizona 85721–0092, USA
[2]SETI Institute/NASA Ames Research Center, MS 245-3 Moffett Field, California 94035–1000, USA
[3]Geofluids Research Group, Department of Geology and Petroleum Geology, University of Aberdeen, Aberdeen, AB24 3UE, UK
[4]Planetary and Space Science Centre, Department of Geology, University of New Brunswick,
2 Bailey Drive, Fredericton, New Brunswick E3B 5A3, Canada
[†]Canadian Space Agency, 6767 Route de l'Aéroport, Saint-Hubert, Quebec, J3Y 8Y9, Canada
[*]Corresponding author. E-mail: osinski@lycos.com

(Received 14 April 2004; revision accepted 25 October 2004)

Abstract–The well-preserved state and excellent exposure at the 39 Ma Haughton impact structure, 23 km in diameter, allows a clearer picture to be made of the nature and distribution of hydrothermal deposits within mid-size complex impact craters. A moderate- to low-temperature hydrothermal system was generated at Haughton by the interaction of groundwaters with the hot impact melt breccias that filled the interior of the crater. Four distinct settings and styles of hydrothermal mineralization are recognized at Haughton: a) vugs and veins within the impact melt breccias, with an increase in intensity of alteration towards the base; b) cementation of brecciated lithologies in the interior of the central uplift; c) intense veining around the heavily faulted and fractured outer margin of the central uplift; and d) hydrothermal pipe structures or gossans and mineralization along fault surfaces around the faulted crater rim. Each setting is associated with a different suite of hydrothermal minerals that were deposited at different stages in the development of the hydrothermal system. Minor, early quartz precipitation in the impact melt breccias was followed by the deposition of calcite and marcasite within cavities and fractures, plus minor celestite, barite, and fluorite. This occurred at temperatures of at least 200 °C and down to ~100–120 °C. Hydrothermal circulation through the faulted crater rim with the deposition of calcite, quartz, marcasite, and pyrite, occurred at similar temperatures. Quartz mineralization within breccias of the interior of the central uplift occurred in two distinct episodes (~250 down to ~90 °C, and <60 °C). With continued cooling (<90 °C), calcite and quartz were precipitated in vugs and veins within the impact melt breccias. Calcite veining around the outer margin of the central uplift occurred at temperatures of ~150 °C down to <60 °C. Mobilization of hydrocarbons from the country rocks occurred during formation of the higher temperature calcite veins (>80 °C). Appreciation of the structural features of impact craters has proven to be key to understanding the distribution of hydrothermal deposits at Haughton.

INTRODUCTION

It is well-known that hydrothermal systems will develop anywhere in the Earth's crust where water coexists with a heat source, with magmatic heat sources being predominant on Earth today (e.g., Pirajno 1992; Farmer 2000). A growing body of evidence also suggests that hydrothermal activity is commonplace after the impact of an asteroid or comet into H_2O-rich solid planetary surfaces (see Naumov 2002 for a review). Hypervelocity impact events generate shock pressures and temperatures that can melt and/or heat substantial volumes of target material, providing heat sources capable of sustaining a hydrothermal system. The interaction of impact-melted or impact-heated materials with H_2O in the near surface of a planet will induce a hot rock-water circulatory system that can dissolve, transport, and precipitate various mineral species. This may have important astrobiological implications because hydrothermal systems in general might have provided habitats or "cradles" for the origin and evolution of early life on Earth, and possibly other planets such as Mars (e.g., Shock 1996; Farmer 2000; Kring 2000; Cockell and Lee 2002). Hydrothermal systems are

considered plausible candidates because they represent sites where liquid H_2O, warmth, and dissolved chemicals and nutrients may have been available for extended periods of time. Although impact-induced hydrothermal systems are transient in nature because they lack the usually longer-lasting heat sources that characterize volcanogenic hydrothermal systems, they might still have subsisted long enough to have experienced colonization by thermophilic (heat-loving) microbial communities, particularly in the case of the larger impact structures (Cockell and Lee 2002; Rathbun and Squyres 2002).

Hydrothermal processes have also played an important role in the formation of many different types of mineral and ore deposits (e.g., porphyry copper-molybdenum deposits; tin-tungsten-copper greisen-related deposits; copper-zinc-rich volcanogenic massive sulfide deposits; lead-zinc Mississippi Valley-type deposits) (Pirajno 1992). More recently, it has been noted that impact-induced hydrothermal activity can also result in economic mineralization, as has been the case at the Sudbury (i.e., zinc-lead-copper-silver-gold; Ames et al. 1998) and Vredefort (i.e., gold) (Grieve and Masaitis 1994) impact structures.

Evidence for impact-induced hydrothermal activity has now been recognized at over sixty terrestrial craters (Naumov 2002), from the ~1.8 km diameter Lonar Lake structure, India (e.g., Hagerty and Newsom 2003), to the ~250 km diameter Sudbury structure, Canada (e.g., Ames et al. 1998). Despite the potential economic and astrobiological importance of hydrothermal activity, the nature and distribution of such deposits within impact craters remains poorly studied. This is due, in part, to the lack of surface exposure and preservation of hydrothermal deposits at many terrestrial impact sites. Moreover, it is only in the past few years that hydrothermal activity has been recognized as a fundamental process associated with impact events. The ~39 Ma Haughton impact structure in Canadian High Arctic is well-exposed and well-preserved and, as such, offers an exceptional opportunity to gain a better understanding of the different types of hydrothermal deposits within impact craters and their distribution.

Evidence for hydrothermal activity associated with the Haughton impact event was first recognized during the 1998 and 1999 field seasons of the NASA Haughton-Mars Project (reported in Osinski et al. 2001). Since this discovery, extensive mapping has revealed important new information regarding the nature and distribution of hydrothermal deposits at Haughton (see map insert). This will be described here, along with analytical data that builds upon the studies of Osinski et al. (2001). New fluid inclusion data on a series of hydrothermal minerals is also presented that helps to constrain the temperature conditions during post-impact hydrothermal activity. This data will be discussed and synthesized with new work on the impactites (Osinski and Spray 2001, 2003; Osinski et al. 2005a) and tectonics (Osinski and Spray 2005) of Haughton. Collectively, these studies enable an improved model for the impact-induced hydrothermal system at Haughton to be presented.

GEOLOGICAL SETTING OF THE HAUGHTON IMPACT STRUCTURE

Haughton is a well-preserved complex impact structure 23 km in diameter that is situated on Devon Island in the Canadian Arctic Archipelago (75°22′N, 89°41′W). The impact event occurred ~39 Myr ago (Sherlock et al. 2005), in a target comprising ~1880 m of Lower Paleozoic sedimentary rocks of the Arctic Platform, overlying Precambrian metamorphic basement of the Canadian Shield (Thorsteinsson and Mayr 1987; Osinski et al. 2005b). The unmetamorphosed sedimentary succession consists of thick units of dolomite and limestone, with subordinate evaporite horizons and minor shales and sandstones (Thorsteinsson and Mayr 1987).

Allochthonous crater-fill deposits form a virtually continuous ~54 km^2 unit covering the central area of the structure (Fig. 1) (Osinski et al. 2005a). Recent field studies and analytical scanning electron microscopy indicate that these rocks are carbonate-rich impact melt breccias or clast-rich impact melt rocks (Osinski and Spray 2001, 2003; Osinski et al. 2005a). The impact melt breccias have a maximum current thickness of ~125 m, although the presence of this unit up to ~140 m above the central topographic low area suggests that they originally completely occupied the central area to depths of 200 m or more (Osinski et al. 2005a). The present-day exposure of the allochthonous crater-fill deposits, therefore, represents a minimum. The pale gray-weathering rocks comprise variably shocked mineral and lithic clasts set within a groundmass of calcite + silicate glass ± anhydrite (Osinski et al. 2005a). The lithic clasts are typically angular and are predominantly dolomite and limestone, with minor sandstones, shales, and evaporites, and subordinate lithologies from the crystalline basement (Metzler et al. 1988).

Post-impact lacustrine sediments of the Haughton Formation occupy the central part of the structure (Hickey et al. 1988) (Fig. 1). These sediments were laid down in a crater lake and consist of dolomitic silts and muds with subordinate fine-grained dolomitic sands. Recent field studies suggest that the Haughton Formation was deposited $>10^4$–10^6 yr following the impact event, following a period of erosion during which significant quantities of impact melt breccias and the bulk of any original intra-crater sediments were removed (Osinski and Lee 2005).

SAMPLES AND ANALYTICAL TECHNIQUES

Over 100 samples of hydrothermally altered rocks were collected from around the Haughton impact structure. Polished thin sections were investigated using a JEOL 6400

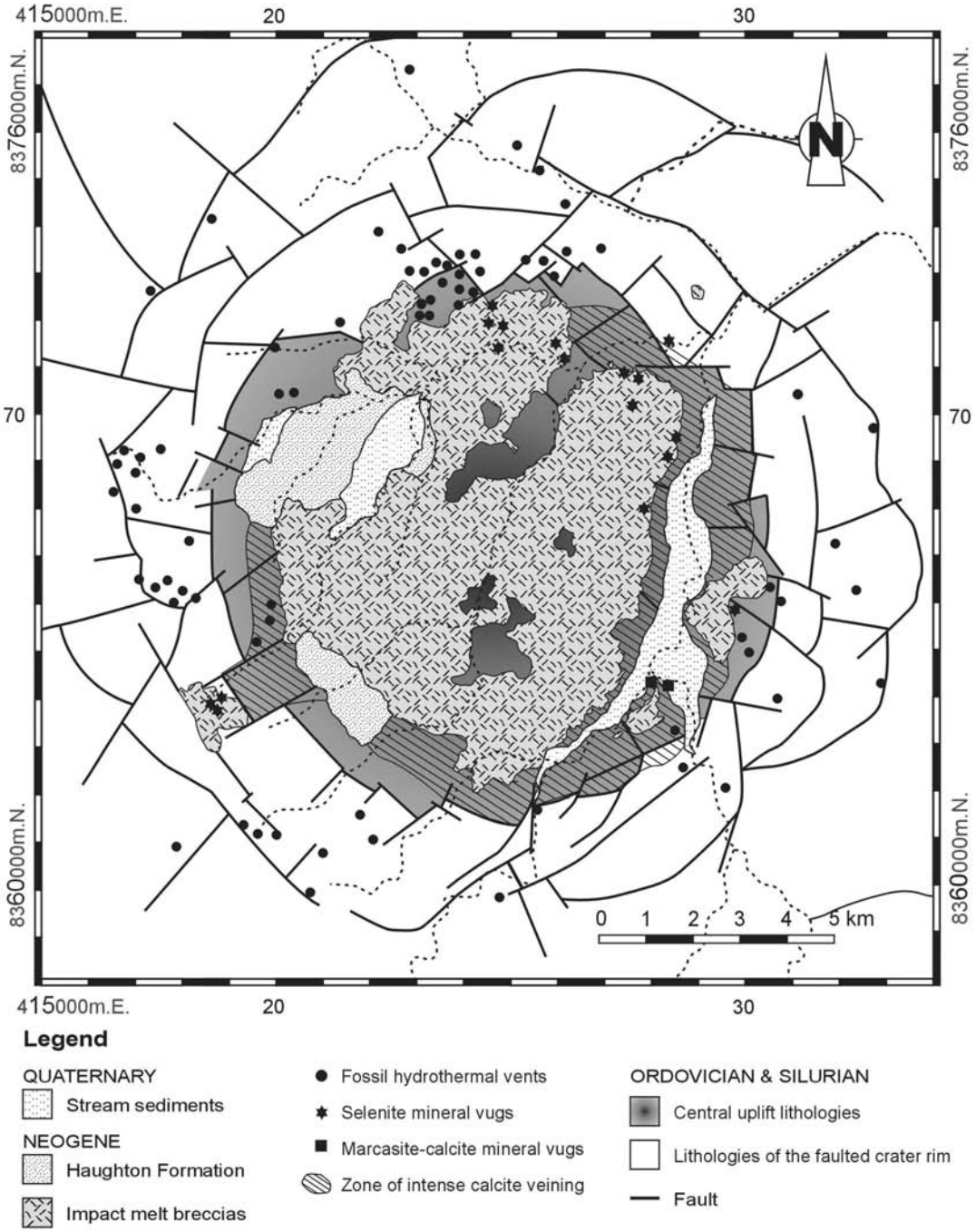

Fig. 1. A simplified geological map of the Haughton impact structure showing the location of various types of hydrothermal deposits. See the map insert for a more detailed version.

digital scanning electron microscope (SEM). The SEM was equipped with a Link Analytical eXL energy dispersive spectrometer (EDS) and Si(Li) LZ-4 Pentafet detector. Beam operating conditions were 15 kV and 2.5 nA at a working distance of 37 mm and count times of 100 sec. SEM data were reduced using a ZAF procedure incorporated into the operating system and calibrated using a multi-element standards block (Type 202-52) produced by the C.M. Taylor Corporation of Sunnyvale, California, USA. SEM backscattered electron (BSE) imagery was used to investigate the microtextures of the hydrothermal phases. The presence or absence of hydrothermal phases was also recorded during the study of >150 samples of impactites (Osinski et al. 2005a). X-ray diffraction (XRD) was performed on powdered samples using a Philips 1710 diffractometer and generator, with operating conditions of 40 kV and 20 mA.

Fluid inclusion studies were carried out at the Geofluids Research Group, University of Aberdeen, UK. Fluid inclusions are a sample of fluid trapped during crystal growth (primary inclusions), or at some later time along fractures (secondary inclusions), after the crystal has formed (Roedder 1981). Non-destructive freezing and heating experiments were performed on polished wafers using a Linkham THM600 heating-freezing stage attached to an Olympus BH-2 petrographic microscope. Organic chemicals of known melting point were used as standards. Fluorescence under UV light was determined using a Nikon Eclipse 600 microscope with a UV-2a filter block. The temperature of homogenization (Th) was recorded on disappearance of the vapor bubble. Homogenization occurred into the liquid state for all (liquid + vapor) inclusions. Freezing studies were used to determine the salinity of the inclusions by measuring the final ice melting temperature (Tm) on reheating the frozen inclusion. The depression of the freezing point of water is directly proportional to the amount of salt in solution. This varies, however, according to the nature of the salt present; therefore, Tm is conventionally reported as weight% NaCl equivalent (Shepherd et al. 1985).

LOCATION, DISTRIBUTION AND NATURE OF HYDROTHERMAL DEPOSITS

Detailed 1:10,000 to 1:25,000 scale mapping carried out over the course of five field seasons reveals a series of distinct hydrothermal deposits at Haughton, each associated with different structural/stratigraphic settings (Fig. 1; map insert).

Mineralization within Crater-Fill Impact Melt Breccias

Hydrothermal alteration assemblages at Haughton are typically restricted to the lower ~20–50 m of the crater-fill impact melt breccia unit and occur as open-space cavity and fracture fillings. Three distinct alteration types identified within impact melt breccias are marcasite-calcite, calcite, and selenite (Osinski et al. 2001), with minor quartz-filled vugs and veins.

Sulfide-Carbonate Mineralization

The largest sulfide deposits occur at two closely spaced localities in a well-exposed cliff section along the Haughton River valley, in the southeastern sector of the structure (Fig. 1) (Osinski et al. 2001). The irregularly shaped vugs are 5–10 m^3 in volume, with the hydrothermal minerals lining the interior surface of the cavity walls (Fig. 2a). Both outcrops are <5–10 m above the basal contact of the crater-fill melt breccias with the underlying pre-impact target rocks. XRD and EDS analysis indicate that the hydrothermal phases are, in decreasing order of abundance, calcite ($CaCO_3$), marcasite (FeS_2), fibroferrite ($Fe(SO_4)(OH).5H_2O$), celestite ($SrSO_4$), barite ($BaSO_4$), fluorite (CaF_2), and quartz (SiO_2) (Figs. 3a–c; Table 1). In addition, ~0.5–2.0 mm thick calcite-marcasite veins have been recognized in four out of more than 150 samples of impact melt breccias studied (Fig. 3d). Field studies, together with SEM backscattered electron imagery, reveal that marcasite occurs in several different forms and settings and is usually the last precipitating phase (Figs. 3a–d), although clear, coarse-grained calcite and fibroferrite were observed after marcasite on the surfaces of some samples (Osinski et al. 2001). It is notable that quartz always occurs as isolated, relatively large grains (~1 mm long), enclosed in calcite, and possessing highly corroded crystal faces. Abundant two-phase (liquid + vapor) fluid inclusions, both primary and secondary, are present in this late stage calcite (e.g., sample 99-135) (Table 2). Fluid inclusions also occur in fine-grained calcite associated the marcasite, but are too small to accurately measure.

Carbonate Mineralization

Large calcite vugs up to ~15 cm across occur within <10–60 m from the base of the impact melt breccia layer. These vugs comprise large (up to ~7 mm long), clear, euhedral calcite crystals projecting into a void (i.e., a typical open-space filling texture). Thin veins of calcite, ~0.5–2.5 mm thick, have also been recognized in 8 out of more than 150 samples of impact melt breccias studied. These veins cross-cut clasts and groundmass phases (e.g., silicate glass, calcite) (Fig. 3e). Two-phase (liquid + vapor) and one-phase (liquid-filled) primary fluid inclusions are common in the vuggy calcite (e.g., sample 092) (Table 2).

Quartz Mineralization

Quartz vugs, very similar in their mode of occurrence to the calcite vugs described above, are present in the lower levels of the impact melt breccia layer, although they are less common than their carbonate counterparts and of smaller size (<8–10 cm across). The large majority of fluid inclusions in the quartz are one-phase (liquid-filled). However, sufficient two-phase (liquid + vapor) primary fluid inclusions were recognized to allow non-destructive heating experiments to be carried out (e.g., sample 091) (Table 2).

Sulfate Mineralization

Field mapping reveals that selenite ($CaSO_4.2H_2O$), a transparent variety of gypsum, is widespread throughout the lower levels of the crater-fill impact melt breccias (Fig. 1; map insert). It is notable that the majority of the mapped occurrences of selenite occur in the eastern quadrants (Fig. 1). Selenite occurs both as large tabular plates from 0.1 m^2 to 1 m^2, and as single, well-formed prismatic crystals growing on clasts within the breccia (Fig. 2b) (Osinski et al 2001). Veins of selenite (~1–10 mm thick) are also common in the basal impact melt breccias (Fig. 3f) (Osinski and Spray 2003),

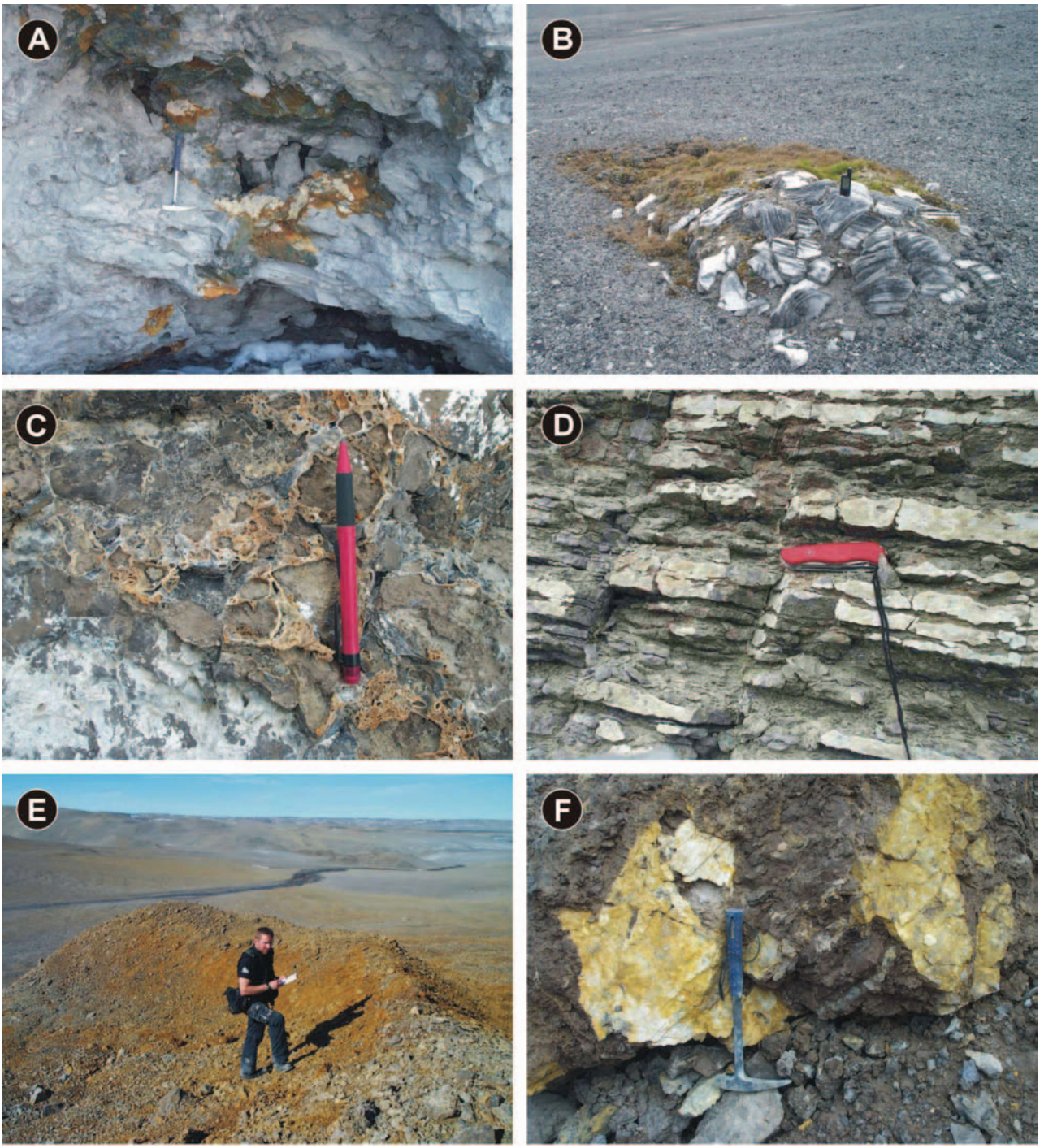

Fig. 2. Field photographs showing the different types of hydrothermal alteration at Haughton. a) Intra-impact melt breccia marcasite (green) and calcite mineralization. Pale yellow accumulations of fibroferrite can be seen to the right of the rock hammer point (40 cm long). 428,110 m.E. 8,364,341 m.N. b) Eroded selenite deposit within the impact melt breccias. A 15 cm high GPS is shown for scale. 424,772 m.E. 8,371,440 m.N. c) Quartz-cemented brecciated carbonates of the Eleanor River Formation in the central uplift at Haughton. A 14 cm long pencil is shown for scale. 425, 821 m.E. 8,371,650 m.N. d) An image showing two sets of calcite veins (~095/70 S and ~155/70 N) cross-cutting limestones of the Bay Fiord Formation in the outer edge of the central uplift. One set is in the plane of the image, while the other is sub-vertical and is approximately perpendicular to the orientation of the image (arrows). A 10 cm long penknife is shown for scale. 426,140 m.E. 8,362,201 m.N. e) The primary author standing within an eroded hydrothermal pipe structure characterized by Fe-hydroxide alteration of the carbonate wall rocks. 419,830 m.E. 8,365,602 m.N. f) A field photograph of two sub-parallel fault surfaces along which calcite mineralization (pale yellow) has occurred. A 40 cm long rock hammer is shown for scale. 424,890 m.E. 8,360,903 m.N.

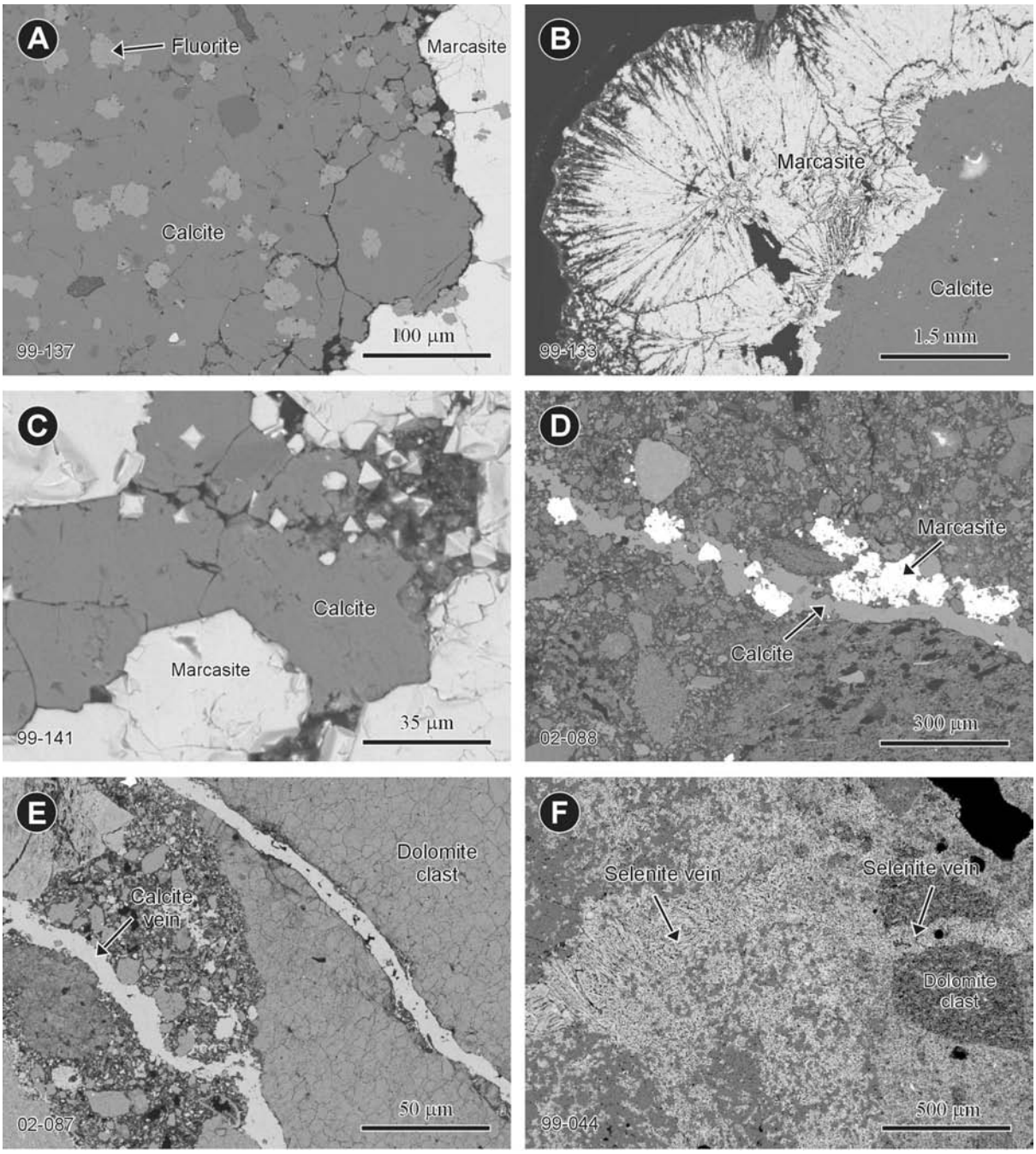

Fig. 3. Backscattered electron (BSE) photomicrographs of hydrothermal alteration products within impact melt breccias. (a) through (c) show a series of BSE images of marcasite-calcite vugs showing the different forms and settings of marcasite. In detail: a) An individual grain of marcasite in a groundmass of hydrothermal calcite and fluorite. b) A layer of radiating marcasite crystals projecting into a void that form a coating on calcite. c) Euhedral to subhedral marcasite grains in a groundmass of hydrothermal calcite. Note the individual tetragonal octahedra in a micro-cavity in the upper right of the image. d) A hydrothermal marcasite-calcite vein that cross-cuts the silicate glass-calcite groundmass of the impact melt breccias. e) Two sub-parallel hydrothermal veins of calcite that cross-cut clasts and groundmass phases in the impact melt breccias. f) As with calcite veins, hydrothermal selenite veins cross-cut both clasts and groundmass phases in the impact melt breccias (cf. Osinski and Spray 2003).

and in uplifted blocks of the Bay Fiord Formation evaporites that lie directly beneath the impact melt breccias. One-phase (liquid-filled) primary fluid inclusions are common in these large selenite crystals (Fig. 4a; Table 2).

Mineralized Breccias in the Interior of the Central Uplift

Hydrothermal alteration associated with the central uplift at Haughton is generally restricted to its outer margins

Table 1. Average composition of selected post-impact hydrothermal phases at Haughton.[a]

Sample #	99-136		99-135		99-133		99-135		02-087		02-088		00-258b	
Phase	Marcasite		Calcite		Celestite		Barite		Calcite		Calcite		Selenite	
Number of analyses	7		10		4		5		5		5		7	
Description	Crust		Interstitial		Interstitial		Interstitial		Vein		Vein		Vein	
	wt%	s.d.	wt%	s.d.	wt%	s.d.	wt%	s.d.	wt%	s.d.	wt%	s.d.	wt%	s.d.
SiO_2	–	–	0.20	0.48	–	n.d.	–	n.d.	0.04	0.12	0.02	0.08	–	n.d.
FeO	33.84	0.52	–	n.d.	0.09	0.34	–	n.d.	0.15	n.d.	0.02	0.07	–	n.d.
MgO	–	–	0.21	0.28	–	n.d.	–	n.d.	53.43	0.41	0.51	0.13	–	n.d.
CaO	–	–	54.73	1.74	0.58	0.40	0.35	0.73	–	1.20	53.14	1.70	32.44	0.76
Na_2O	–	–	0.04	0.18	–	n.d.	0.45	0.65	–	n.d.	–	n.d.	–	n.d.
K_2O	–	–	–	n.d.	–	n.d.	–	n.d.	0.04	n.d.	–	n.d.	–	n.d.
SO_3	65.97	0.14	–	n.d.	43.31	1.11	33.73	0.73	–	0.17	–	n.d.	47.33	1.16
BaO	–	–	–	n.d.	1.03	3.34	63.03	4.35	–	n.d.	–	n.d.	–	n.d.
SrO	–	–	–	n.d.	55.13	2.88	2.64	3.90	–	n.d.	–	n.d.	–	n.d.
Cl	–	–	–	n.d.	–	n.d.	0.45	0.92	0.15	n.d.	–	n.d.	–	n.d.
Total	99.81	0.46	55.18	1.51	100.14	1.32	100.65	1.37	53.61	1.52	53.69	1.59	79.77	1.74

[a]Cr, Ni, P, and Ti were below detection for all analyses. Abbreviations: wt% = mean composition in weight%; s.d. = standard deviation (2σ); n.d. = not determined. The first four groups of analyses are from a calcite-marcasite vug within the impact melt breccias. The last three groups of analyses are from hydrothermal veins from the impact melt breccias.

Table 2. Summary of fluid inclusion data for representative samples of hydrothermal deposits at Haughton.[a]

Sample #	UTM Position Easting	UTM Position Northing	Location in crater	Setting	Host mineral	Inclusion type	Size range (μm)	Fill[b]	Th (°C)	Tm (°C)	Salinity (wt% NaCl eq.)
99-063	425,010	8,369,020	Interior of central uplift	Cem. breccia	Cl. Qtz.	P1	2–6	1	n.d.[c]	n.d.[d]	n.d.[d]
99-091	429,630	8,372,930	Impact melt breccias	Vug	Quartz	P1	2–6	1	n.d.[c]	n.d.[d]	n.d.[d]
				Vug	Quartz	P2	2–5	0.97–0.98	71.0–91.6	–0.1–0.5	0.2–0.7
99-092	428,500	8,369,760	Impact melt breccias	Vug	Calcite	P1	2–6	1	n.d.[c]	n.d.[d]	n.d.[d]
				Vug	Calcite	P2	2–5	0.96–0.98	70.1–94.9	n.d.[d]	n.d.[d]
99-104	429,460	8,370,350	Periphery of central uplift	Vein	Tr. Cal.	P1	2–8	1	n.d.[c]	–0.2–1.1	0.4–2.0
				Vein	Tr. Cal.	P2	2–8	0.95–0.98	81.4–144.4	–0.4–1.4	0.7–2.4
				Vein	Cl. Cal.	P2,S2, HC	3–25	0.94–0.96	141.3–174.8	n.d.[d]	n.d.[c]
99-135	428,000	8,364,390	Impact melt breccias	Vug	Calcite	P2	2–4	0.92–0.96	117.7–210.1	–0.1–0.6	0.2–1.1
				Vug	Calcite	S2	3–4	0.90–0.96	143.5–184.8	n.d.[d]	n.d.[d]
00-098	417,750	8,368,430	Periphery of central uplift	Vein (LS)	Cl. Cal.	P1	2–3	1	n.d.c	–0.4–1.0	0.7–2.1
				Vein (ES)	Cl. Cal.	S2, HC	2–4	0.95–0.96	91.0–142.6	n.d.d	n.d.[d]
				Host rock	Cl. Cal.	S2, HC	2–4	0.94–0.96	91.0–142.6	n.d.	n.d.
				Host rock	Br. Cal.	S2	2–3	0.95–0.96	83.8–118.3	–13.5	17.4
00-136	420,570	8,359,890	Periphery of central uplift	Vein	Calcite	P2	2–3	0.94–0.96	136.6–142.8	–0.3–0.4	0.7
00-258	427,830	8,367,980	Impact melt breccias	Vug	Selenite	P1	2–5	1	n.d.[c]	–0.1–3.7	0.2–6.0
02-035	418,650	8,363,780	Impact melt breccias	Vug	Selenite	P1, S1	2–5	1	n.d.[c]	–0.5–0.8	0.7–1.4
02-048	426,540	8,361,980	Periphery of central uplift	Vein	Cl. Cal.	P2	2	0.97–0.98	67.9–85.1	–1.1–2.0	1.9–3.4
				Vein	Br. Cal.	S2, HC	2–3	0.95–0.96	62.7–101.4	n.d.[d]	n.d.d
02-121	425,820	8,371,650	Interior of central uplift	Cem. breccia	Ml. Qtz.	P2	3–11	0.92–0.97	84.3–249.8	n.d.[d]	n.d.d
				Cem. breccia	Cl. Qtz.	P1	3–4	1	n.d.c	–0.2–0.8	0.4–1.4
02-248	419,660	8,373,870	Crater rim region	Unshocked	Dolomite	P2	2–6	0.96–0.97	64.5–118.7	–13.4–14.6	17.3–18.3
				Target rock	Dolomite	P2, HC	2–5	0.95–0.98	62.7–101.4	n.d.	n.d.

[a]Abbreviations: Th = temperature of homogenization; Tm = final ice melting temperature; P = primary; S = secondary; 1 = one-phase; 2 = two-phase; HC = hydrocarbon-bearing; n.d. = not determinable; Cal. = calcite; Qtz. = quartz; Cem. = cemented; Cl. clear; Br. = brown; Tr. = translucent; Ml. = milky; ES = early stage; LS = late stage.

[b]The degree of fill is defined as the volumetric proportion of liquid relative to the total volume of the inclusion.

[c] It is not possible to carry out heating experiments on one-phase fluid inclusions.

[d] It is not possible to carry out heating experiments on one-phase fluid inclusions.

(see below). However, minor mineralization has been observed and studied at three locations in uplifted strata of the Eleanor River Formation in the center of the crater (Figs. 1 and 2c; map insert). Quartz is the only hydrothermal mineral observed and its occurrence is typically limited to the cementation of highly fractured, and brecciated carbonate lithologies (Fig. 2c). Several <0.5–1.0 mm thick veins have also been observed. Two phases of quartz are distinguishable in hand specimen and using plane-polarized light: a cream–pale blue colored milky variety and clear quartz that cross-cuts the former. Primary fluid inclusions are present within both varieties (e.g., samples 99-063 and 02-121) (Table 2). In the volumetrically significant clear quartz, the inclusions are one-phase (liquid filled), whereas in the milky quartz, two-phase (liquid + vapor) inclusions are present, which are also larger in size than the inclusions in the clear quartz (Table 2).

Veining Around the Outer Margin of the Central Uplift

A zone of (sub-) vertical faults and bedding occurs at a radial distance of 5.5–6.0 km from the center of the crater (Fig. 1) (Osinski and Spray 2005). These highly fractured rocks contain a pervasive network of thin (<2–5 mm thick) calcite veins that are notably more common in the eastern and southern regions (Figs. 1 and 2d). Two phases of calcite are discernible under plane polarized light: clear calcite and a translucent, sometimes pale brown variety. Abundant fluid inclusions are present in both types of calcite; however, the type of inclusions always differs between the two varieties (e.g., samples 99-104 and 02-048) (Table 2). It is notable that fluid inclusions of liquid hydrocarbon have been found in both calcite types. These inclusions are typically two-phase with a high degree of liquid fill. Hydrocarbon-bearing fluid inclusions are both primary and secondary (in cross-cutting trails), up to ~25 μm in diameter, and fluoresce yellow-green to blue-white under ultraviolet light (Fig. 4b; Table 2) (Parnell et al. 2003). In sample 99-104, the fluorescing inclusions of liquid hydrocarbon are far more abundant in areas in close proximity to clasts of argillaceous host rock that are suspended in the veins. Secondary, two-phase fluid inclusions of liquid hydrocarbon also occur within the carbonate crystals of the vein host rock (e.g., sample 99-098) (Table 2). Similar hydrocarbon-bearing fluid inclusions are present within dolomite crystals of an unshocked reference sample collected near the crater rim (sample 02-248) (Table 2). These inclusions fluoresce yellow and appear to have been trapped during crystal growth (Parnell et al. 2003).

Hydrothermal Pipe Structures Around the Crater Periphery

Detailed field mapping has revealed the presence of over seventy hydrothermal pipe structures or gossans at Haughton (Fig. 1; map insert). It is notable that they are developed exclusively around the rim of the impact structure where faulting occurs, and have not been found developed in the

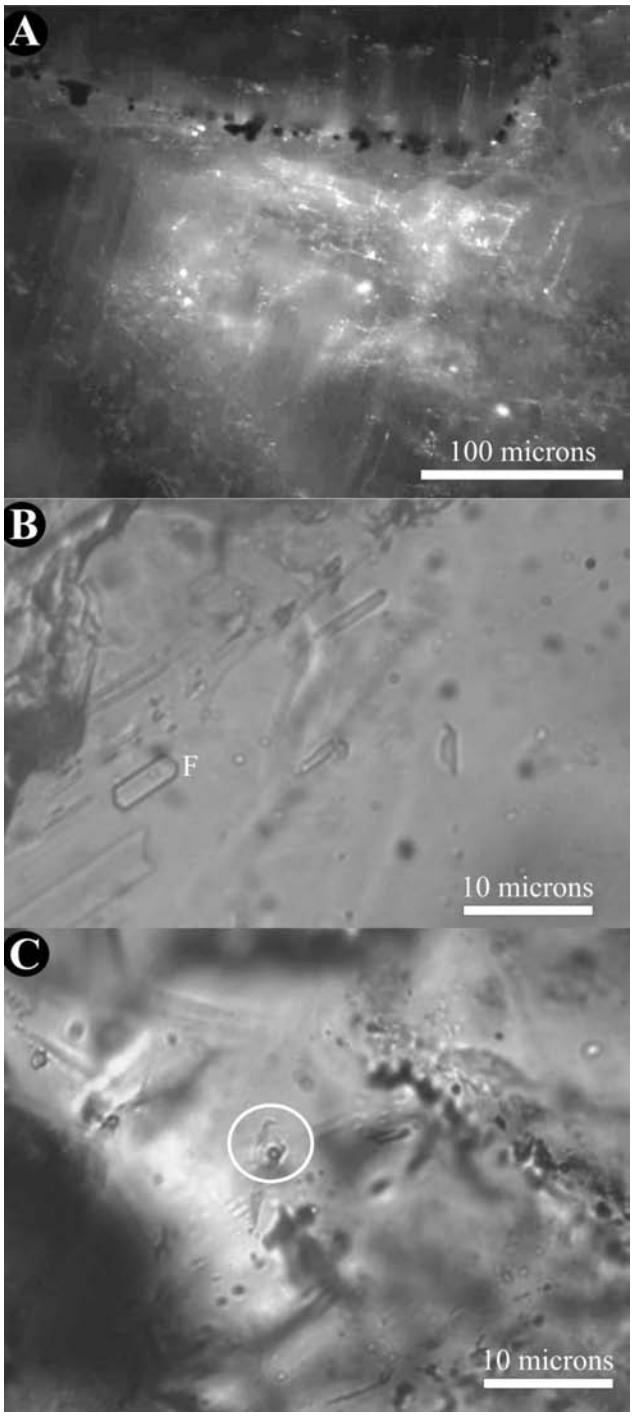

Fig. 4. Photomicrographs of fluid inclusions. a) Two-phase hydrocarbon inclusions within calcite. See Fig. 5c for results of fluid inclusion studies. b) Monophase inclusions (F) in selenite from a vug impact melt breccias, Gemini Hills. c) Two-phase primary aqueous inclusions in quartz from the interior of the central uplift at Haughton.

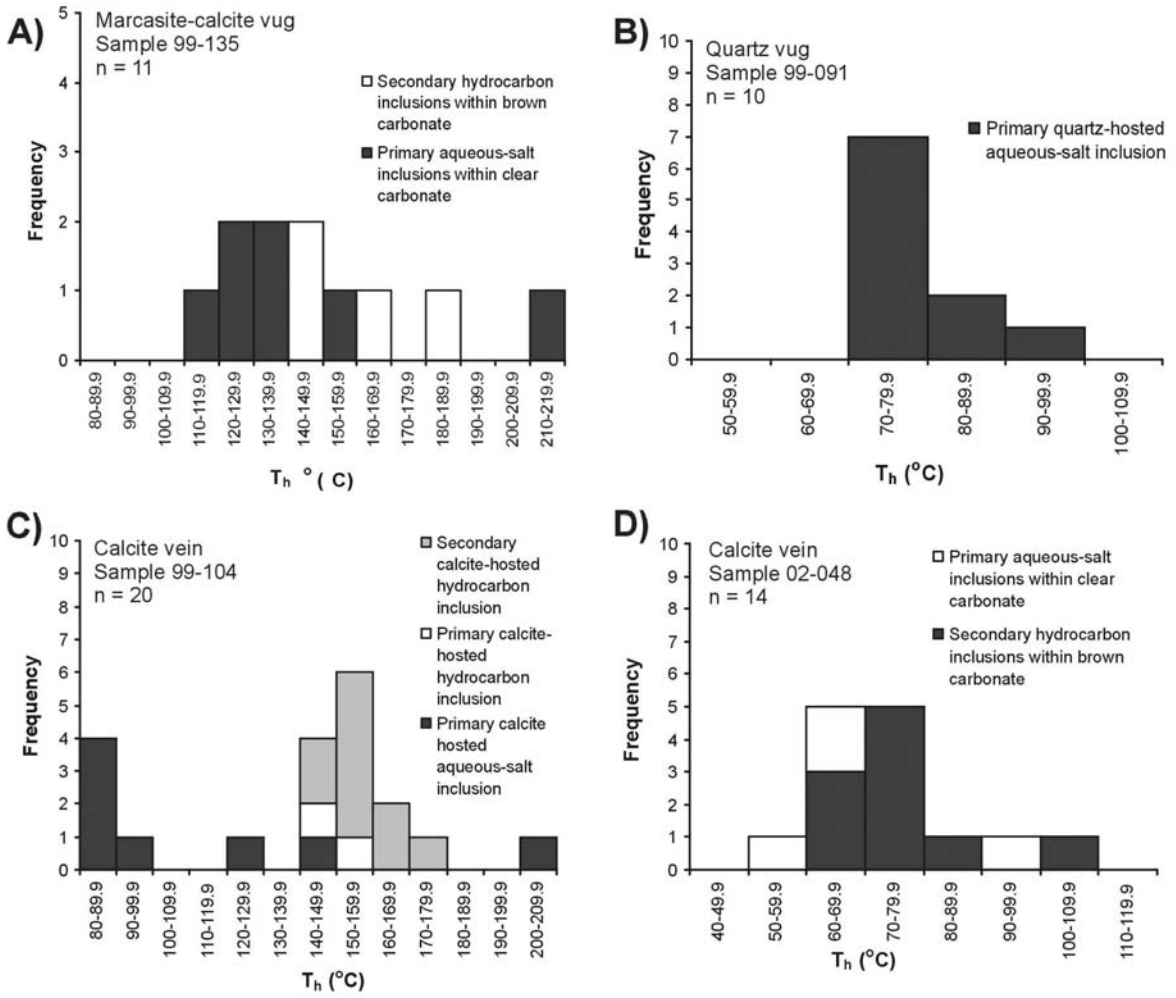

Fig. 5. Frequency plots of fluid inclusion homogenization temperatures (Th) from representative hydrothermal phases at Haughton. a) Results from fluid inclusion studies of calcite associated with marcasite in the impact melt breccias. b) Isolated quartz vug from the impact melt breccias. c) and d) Calcite veins from the periphery of the central uplift. The hydrocarbon-bearing veins (c) record higher temperatures than the hydrocarbon-free veins (d).

crater-fill impactites, or in central uplift lithologies (Fig. 1). These features are, therefore, different to the degassing pipes found at the Ries impact structure, Germany, that are developed exclusively within impactites (Newsom et al. 1986). The highly brecciated, cylindrical pipe-like structures at Haughton are typically 1–5 m in diameter and are exposed over vertical lengths of up to 20 m, although the quality of exposure is generally poor (Fig. 2e) (Osinski et al. 2001). They are always sub-vertical and are characterized by pronounced Fe-hydroxide (goethite, FeO(OH)) alteration of the carbonate wall rocks. The brecciated interior of the pipes are lined and/or cemented with either calcite or quartz and series of sulfide minerals (marcasite + pyrite ± chalcopyrite ($CuFeS_2$)). The textural relationships between the various sulfide minerals is unknown, due to highly friable and fine-grained nature of the samples in which they have been documented. At higher structural levels, the pipe structures are characterized by being very porous with cavities and fractures lined by calcite and/or gypsum.

Mineralization Along Faults and Fractures in the Crater Rim Area

Fault surfaces within the heavily faulted rim of the Haughton structure are frequently lined by cream or pale yellow calcite (Fig. 2f). Fe-hydroxide and/or oxide alteration of fault surfaces can also occur. Occasionally, fault surfaces display crystal fiber lineations produced by the preferred directional growth of calcite or quartz during movement (Osinski et al. 2001). The presence of crystal fiber lineations indicates that fluids migrated along the faults after the impact event.

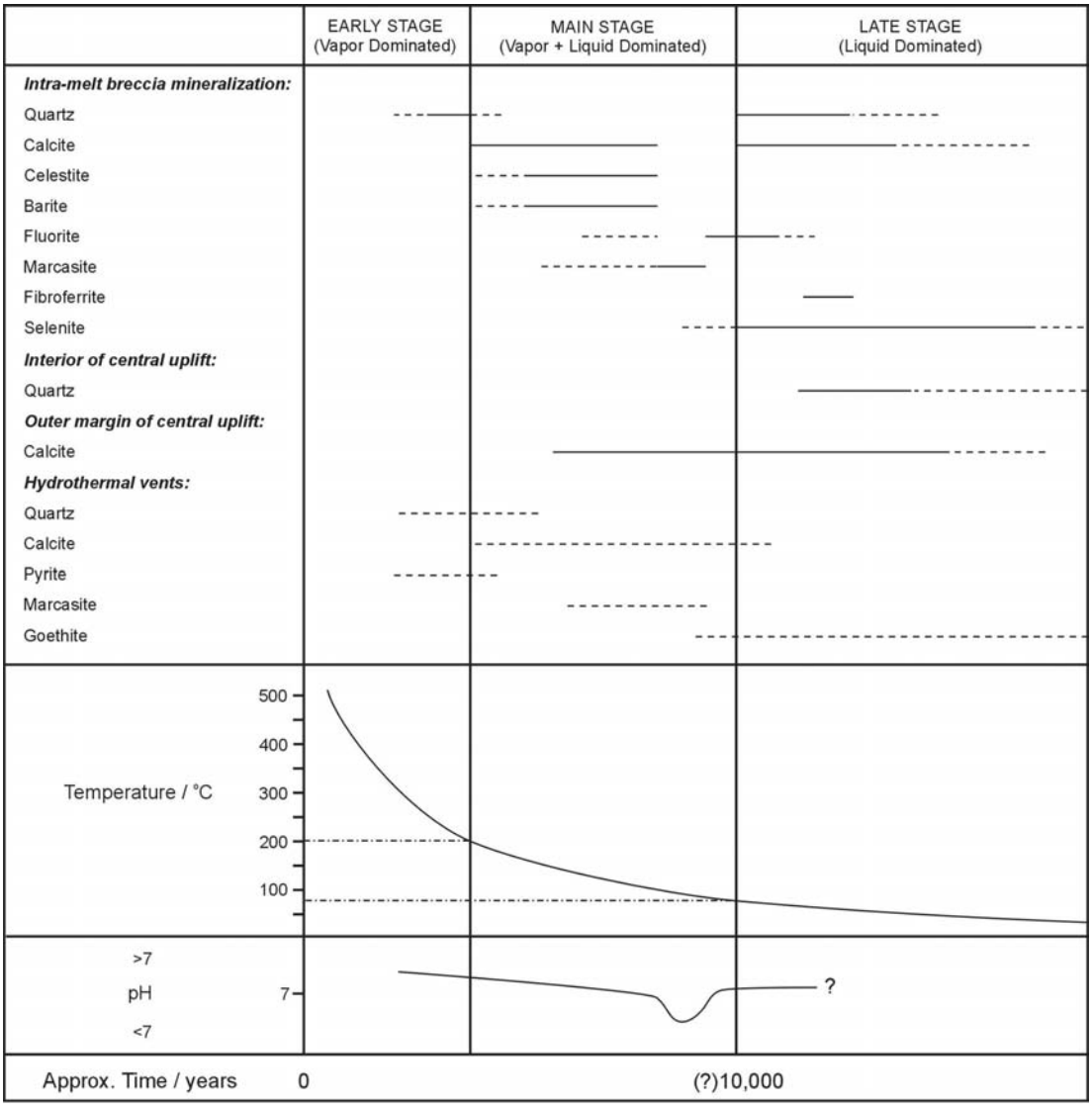

Fig. 6. The paragenetic sequence for hydrothermal mineralization within the Haughton impact structure. Quartz appears to have been the first mineral to precipitate from the hydrothermal fluids, probably at temperatures of ~340–200 °C. Calcite precipitation followed during the main stage of hydrothermal activity, associated with marcasite, celestite, and barite, in the impact melt breccias at temperatures of ~210 down to ~120 °C. The formation and mineralization of the hydrothermal pipe structures around the crater rim area was probably initiated in a similar temperature range. Calcite veining and mobilization of hydrocarbons occurred shortly thereafter in the faulted periphery of the central uplift at temperatures of ~150–80 °C. A decrease in the pH of the hydrothermal solutions circulating through the impact melt breccias led to deposition of radiating marcasite crystals that typically form a crust on calcite. The resumption in calcite precipitation during the late stage of hydrothermal activity, in association with a substantial increase in the amount of fluorite deposited, was associated with an increase in pH. Late-stage deposition of fibroferrite occurred on some marcasite surfaces. The final stages of hydrothermal alteration at Haughton consisted of widespread selenite and minor quartz and calcite deposition in cavities near the base of the impact melt breccias. Calcite veining, without the involvement of hydrocarbons, also continued down to ~60 °C around the periphery of the central uplift. Modified from Osinski et al. (2001) using additional data from this study.

GEOTHERMOMETRY AND MINERAL PARAGENESIS

New fluid inclusion studies combined with data on mineral paragenesis (Osinski et al. 2001) allows a more accurate model of the hydrothermal system at Haughton to be developed.

Sulfide-Carbonate Mineralization

Marcasite associated with calcite occurs predominantly as open-space fillings in cavities and fractures within the crater-fill impact melt breccias. Minor sulfide-carbonate mineralization also occurs within the hydrothermal pipe structures. Field and analytical data from Haughton (Osinski

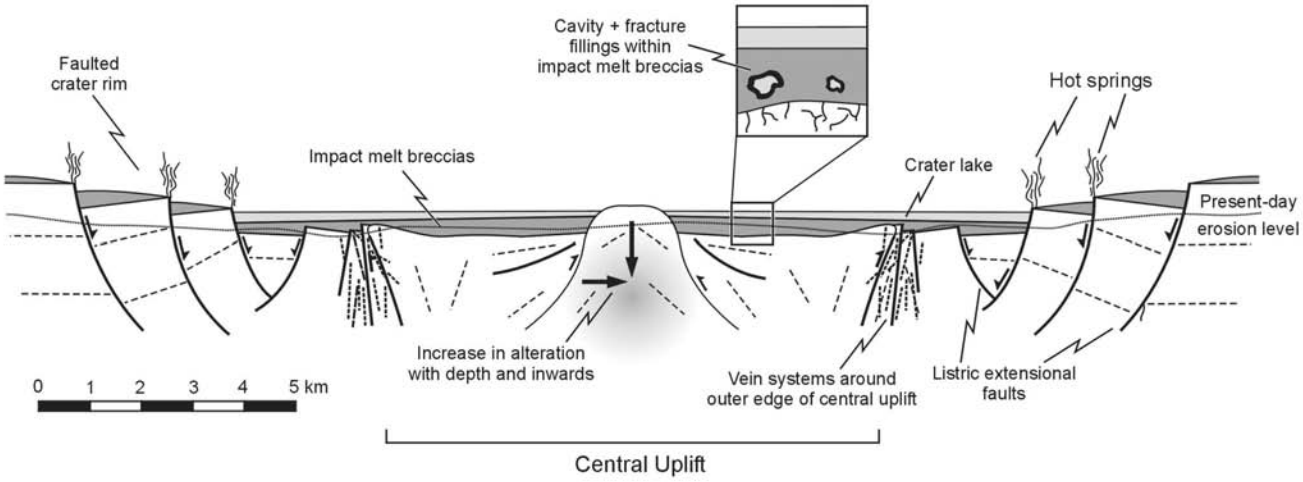

Fig. 7. A schematic cross-section showing the nature of the hydrothermal system shortly after commencement of hydrothermal activity following the Haughton impact event. See text for details.

et al. 2001), coupled with experimental data on marcasite formation (Murowchick and Barnes 1986; Goldhaber and Stanton 1987; Schoonen and Barnes 1991a, 1991b, 1991c), suggests that the conditions of formation of primary marcasite at Haughton includes: (a) acidic mineralizing fluids with pH <5.0; (b) temperature of deposition >100 to <240 °C; and (c) presence of neutral polysulfide species (H_2S_n) at the site of deposition (i.e., monovalent or divalent polysulfide species would favor pyrite formation, which did not occur within the impact melt breccias at Haughton).

Calcite is the most dominant hydrothermal phase associated with marcasite at Haughton and likely exsolved due to the degassing of CO_2 through boiling, and precipitated by cooling, associated with a rise in pH (Osinski et al. 2001). Fluid inclusion studies performed on late-stage clear calcite (sample 99-135) yield temperatures of homogenization (Th) of primary inclusions of 118–210 °C (Fig. 5a; Table 2). This temperature range represents the final stages of intramelt breccia marcasite-calcite mineralization at this particular locality (Fig. 6), and is consistent with experimental studies (Schoonen and Barnes 1991a, 1991b, 1991c). It is, therefore, likely that marcasite-calcite mineralization commenced at higher temperatures, possibly up to ~240 °C based on the experimental evidence for marcasite formation (see above). By analogy, it is suggested that sulfide-carbonate formation within the hydrothermal pipe structures occurred at similar temperatures.

Calcite Mineralization

In addition to being associated with sulfides (see above), calcite also occurs as monomineralic vugs and veins within impact melt breccias and around the outer margin of the central uplift, and as cement within brecciated pipe structures around the crater periphery.

For calcite vugs within the impact melt breccias, Th of primary fluid inclusions range from ~70 to 95 °C (e.g., Table 2) (sample 99-092). The relationship between this carbonate mineralization and the sulfide-carbonate mineralization is unclear. However, the presence of calcite and calcite-marcasite veins cross-cutting impact melt breccias in the same outcrop would suggest a close temporal and genetic relationship between the two types of mineralization. The presence of abundant one-phase (liquid-filled) fluid inclusions indicates that calcite formation continued down to temperatures of <60 °C within the impact melt breccias.

Fractures around the outer margin of the central uplift are filled with two main varieties of calcite. Calcite veins containing no hydrocarbons record temperatures of ~65–145 °C, with <90 °C being typical (e.g., Fig. 5c; Table 2) (samples 99-104, 00-098, 02-048). Calcite formation continued down to temperatures of <60 °C, as evidenced by abundant one-phase fluid inclusions. Higher temperatures (up to 209 °C) were recorded, but petrographic evidence shows that they are due to stretching of primary fluid inclusions and are therefore not reliable. In contrast, Th of primary inclusions from hydrocarbon-bearing calcite typically ranges from 91 to 175 °C (e.g., Fig. 5c; Table 2) (samples 99-104, 99-098), although one sample yielded slightly lower temperatures (Fig. 5d; Table 2) (sample 02-048). The wide range of Th of the fluid inclusions suggests that calcite veining around the outer margin of the central uplift was relatively long-lived. This is consistent with the presence of several cross-cutting series of veins and the pervasive nature of the veining in places.

Parnell et al. (2003) have shown that liquid hydrocarbons are present in the Lower Paleozoic target lithologies at Haughton, especially dolomites of the Allen Bay Formation (Table 2) (sample 02-248). Fluid inclusion and geochemical data from the dolomites suggest that the dolomite texture and

its enclosed hydrocarbons are a product of deep burial diagenesis at depths of ~3–4 km (Parnell et al. 2003). Thus, it is clear that hydrocarbons at Haughton survived the impact event, at least near the crater rim, and were mobilized and entrained during impact-induced hydrothermal activity (cf. Parnell et al. 2005).

Quartz Mineralization

Quartz vugs within the impact melt breccias at Haughton contain fluid inclusions that yield homogenization temperatures of 71–92 °C with a mean of 78 °C (e.g., Fig. 5b; Table 2) (sample 99-091). One-phase fluid inclusions are also abundant, which indicates that quartz mineralization continued down to <60 °C. Minor quartz is also associated with the sulfide-carbonate mineralization within the impact melt breccias. It is notable that this quartz displays evidence of dissolution (e.g., highly corroded crystal faces), which is unusual and requires special hydrothermal conditions. Moore et al. (2000) suggest that the production of fluids capable of quartz dissolution is only possible in a vapor-dominated hydrothermal system.

The quartz-cemented carbonate breccias within the interior of the central uplift contain two distinct generations of quartz. The early-stage milky quartz contains abundant two-phase (liquid + vapor) fluid inclusions that record a range of T_h from 84 to 250 °C (Table 2) (sample 02-121). It is notable that this milky quartz can also occur as a thin (<1 mm thick) coating, displaying botryoidal textures, on the brecciated central uplift lithologies. These coatings were not amenable to fluid inclusion studies; however, given the high temperatures recorded by other milky quartz varieties, and the distinctive textures displayed by this phase, it is suggested that deposition of milky quartz commenced during an early vapor-dominated stage at temperatures >250 °C (cf. endogenous vapor-dominated hydrothermal systems; e.g., White et al. 1971; Moore et al. 2000, 2002). The preponderance of one-phase (liquid-filled) fluid inclusions in the later cross-cutting clear quartz indicates that this variety formed at temperatures <60 °C. Thus, two distinct episodes of quartz mineralization occurred within the interior of the central uplift.

Sulfate Mineralization

It is known that sulfate minerals can form at low temperatures (<100 °C), which is consistent with the preponderance of one-phase (liquid-filled) fluid inclusions in selenite from the impact melt breccias at Haughton (Fig. 4a). A possible explanation for the precipitation of selenite is the mixing of late-stage hydrothermal fluids with cooler, more oxygenated groundwaters, resulting in an increase in pH and oxidation state of the solution (Osinski et al. 2001). Fluids rich in $CaSO_4$ were almost certainly derived from gypsum and anhydrite beds of the Bay Fiord Formation that underlie the impact melt breccias, which may explain the restriction of selenite mineralization to the lower reaches of the breccia deposits. This is also consistent with the concentration of selenite mineralization in the eastern parts of the impact melt breccia layer, as this mirrors the outcropping of the Bay Fiord Formation evaporites (i.e., Bay Fiord Formation strata only outcrop in the eastern half of the Haughton structure) (map insert). However, it is notable that abundant selenite deposits occur in impact melt breccias preserved in a down-faulted graben in the southwest of the structure (Fig. 1). At this location, Bay Fiord Formation evaporites are currently at a depth of ~300–500 m, indicating the importance of impact-generated faults for fluid flow.

POST-IMPACT HYDROTHERMAL MODEL

The comprehensive post-impact hydrothermal model outlined below for Haughton is based on extensive field, analytical and fluid inclusion studies. This model may also be applicable as a working model for other complex impact structures in the size range ~5–100 km in diameter, particularly in terms of the distribution and style of hydrothermal alteration. However, hydrothermal systems and their deposits are also strongly dependant on host rock composition (e.g., Naumov 2002; Ames et al., Forthcoming). For example, the carbonate- and sulfate-dominated target sequence at Haughton ensured that clays, zeolites, and K-feldspar were not formed (Osinski et al. 2001), in contrast to the typical alteration products of terrestrial impact structures developed in silicate-rich crystalline targets (Naumov 2002). In general, hypervelocity impact events generate structures (e.g., faults, fractures), enhanced permeability, and a heat source(s) that drive and focus hydrothermal fluids, if H_2O is present in the target (cf. Ames et al. 2000).

Early Stage: >200 °C

Impact events generate extreme pressures and temperatures that will disrupt and/or eliminate the original water table in a substantial portion of the target sequence. Following readjustment of the initial or transient crater during the modification stage, the hydrological "void" left by the impact event would cause replacing waters to rise from depth, as well as being drawn in laterally from the water table in the relatively undisturbed rocks surrounding the crater (Fig. 7). The interaction of the re-established hydrosphere with hot impact-generated and impact-heated rocks will create a hydrothermal system within the crater following impact (e.g., Kieffer and Simonds 1980; Newsom 1980; Allen et al. 1982). Some exceptions may occur with small craters and in extreme arid environments (Osinski et al. 2001).

The heat source for the hydrothermal system at Haughton was primarily the hot impact melt breccias that filled the crater interior to depths of >200 m (Osinski et al. 2005a). The initial temperature of these impactites is difficult to estimate; however, impact melts originating from crystalline targets are

generally assumed to be superheated, with initial temperatures >2000 °C (e.g., Grieve et al. 1977). Little is known about the emplacement temperatures of sediment-derived impact melts; however, the presence of immiscible textures between carbonate and SiO_2 glass at Haughton (Osinski et al. 2005a), would suggest initial textures of >1500–2000 °C. Such temperatures are consistent with evidence for high-temperature sediment-derived impact melts from Ries impact structure, Germany (Graup 1999; Osinski 2003; Osinski et al. 2004), although the glassy nature of the silicate phases in the Haughton and Ries impactites indicates subsequent rapid cooling below the liquidus for these melts (~600–900 °C).

Within the country rocks directly below the hot impact melt breccias, more water would be boiled off than could be replaced, resulting in the development of a short-lived vapor-dominated regime (Osinski et al. 2001); whereas at deeper levels, it is likely that a two-phase (vapor + liquid) zone would form. In addition, the re-established, now boiling water table, would be deflected downwards due to heat from the overlying melt breccias (Newsom 1980). Minor quartz deposition within cavities and fractures in the interior of the central uplift and impact melt breccias occurred during this vapor-dominated stage.

Main Stage: ~200–80 °C

Our studies at Haughton have revealed the importance of impact-generated fault systems in governing the location and nature of post-impact hydrothermal alteration (cf. endogenous hydrothermal systems; e.g., Park and MacDiarmid 1975). For example, hydrothermal pipe structures are developed exclusively around the rim of the Haughton structure where faulting occurs, and have not been found developed in the impact melt breccias or in the interior of the central uplift. The concentric listric faults and interconnecting radial faults would have acted as fluid pathways, enabling hot fluids and steam to travel along them (Fig. 7). Hydrothermal fluids were also focused into a zone of intense faulting and fracturing around the periphery of the central uplift (Fig. 7). By analogy with volcanogenic hydrothermal systems, the vapor and liquid phases can travel independently, with liquid phases traveling laterally for several kilometers away from the boiling zone (Nicholson 1993). This is evidenced at Haughton in the form of hydrothermal pipe structures around the periphery of the crater, some several kilometers from the heat source.

The main stage of hydrothermal activity at Haughton would have been characterized by a progressive cooling of the impact melt breccias and the development of a two-phase (vapor + liquid) zone (Osinski et al. 2001). Field and analytical evidence suggests that a simple convection system was developed, with hot liquids and steam rising up and flowing laterally from the boiling water table. These fluids then cooled, and may have been discharged in the outer reaches of the crater, or may have descended for recirculation (Fig. 7). The fluids circulating in a hydrothermal system may be derived from a number of source reservoirs. The low salinities of fluid inclusions in carbonates and quartz (<3 wt% NaCl equivalent) at Haughton suggest that the dominant components of the system were a combination of surface or meteoric waters. Indeed, this appears to be the case for the majority of impact-induced hydrothermal systems formed in continental settings (Naumov 2002). The higher salinities of fluid inclusions from the Paleozoic target rocks (>17 wt% NaCl equivalent) indicate that trapped pore waters did not significantly contribute to the hydrothermal system at Haughton.

Within the impact melt breccias, early quartz precipitation was followed by the deposition of calcite, which continued until the final stages of hydrothermal activity. It is likely that precipitation of calcite occurred due to boiling of the hydrothermal fluids, resulting in the decrease in the concentration of CO_2 in the liquid phase, concomitant with an increase in pH (cf. Nicholson 1993). Marcasite, together with minor celestite, barite, and fluorite were then co-precipitated with calcite in the impact melt breccias at temperatures of ~110–200 °C (Fig. 6). The most likely mechanism for marcasite precipitation within the impact melt breccias was through partial oxidation of H_2S gas in the vapor phase, together with condensation of the steam in more oxygenated groundwaters (Fig. 7) (Osinski et al. 2001).

Fluid flow and precipitation of calcite associated with hydrocarbons in the fractured and faulted margins of the central uplift was initiated in a similar temperature range (~80 to 150 °C). Although evidence from fluid inclusions is lacking, the presence of marcasite and pyrite within the hydrothermal pipe structures would suggest the flow of mineralizing fluids with temperatures on the order of ~100–200 °C in this region during the main stage of hydrothermal activity at Haughton.

Late Stage: <80 °C

The circulation of fluids during the final stages of the hydrothermal system at Haughton was areally extensive. By this time, the impact breccias would have been cooled by conduction with the cooler underlying country rocks, and by convection via waters from an overlying crater lake(s). Calcite mineralization within veins and isolated cavities in impact melt breccias and around the margins of the central uplift, continued down to ~60–90 °C (Fig. 6). This was followed by selenite and quartz deposition in cavities within the impact melt breccias at low temperatures (<60 °C). Selenite deposition likely occurred through the mixing of hydrothermal fluids with cooler, more oxygenated groundwater (Osinski et al. 2001). The abundance of selenite suggests that the fluids were saturated in sulfate ions, most

probably derived from the underlying uplifted Bay Fiord Formation gypsum and anhydrite beds. The higher salinity of fluid inclusions in late-stage selenite (up to ~6 wt% NaCl equivalent) supports this conclusion.

A second episode of quartz mineralization occurred within brecciated lithologies in the interior of the central uplift at temperatures <60 °C. It is important to note that silica-rich (e.g., sandstone) horizons are most common in the oldest Paleozoic target rocks, implying that SiO_2 may have been leached from deeper levels of the stratigraphy (>1400 m). Seismic reflection studies indicate that some of the impact-generated faults penetrate to depths of 1.5 km or more (Scott and Hajnal 1988). These faults may have facilitated SiO_2 transport from depth.

DISCUSSION

Heat Sources in Impact-Induced Hydrothermal Systems

There are three main potential sources of heat for creating impact-generated hydrothermal systems: (a) impact-generated melt rocks and melt-bearing breccias; (b) elevated geothermal gradients in central uplifts; and (c) energy deposited in central uplifts due to the passage of the shock wave. The relative importance of each of these heat sources is not clear at present. Preliminary studies by Daubar and Kring (2001) suggest that impact melt rocks contribute ~10–100 times more energy than elevated geothermal gradients in central uplifts. However, when shock heating is factored in to the models, it appears that the heat contribution from uplifted target rocks is approximately the same as that from impact melt rocks (Thorsos et al. 2001). This is supported by preliminary modeling studies of a 30 km diameter crater, under Martian conditions, which suggest that the heating comes mainly from shock wave propagation combined with the structural uplift of rocks underneath the crater, although this is highly dependant upon the impact conditions (Pierazzo et al. 2005).

For Haughton, with a structural uplift of ~2 km, the elevated geothermal gradient would have provided a maximum temperature of ~70 °C (assuming a geothermal gradient of 30 °C km^{-1} and a surface temperature of ~10 °C). Given such a relatively low temperature, hydrothermal activity at Haughton cannot exclusively be attributed to the elevated geothermal gradient in central uplift (Osinski et al. 2001), although an additional heat component from the passage of the shock wave is likely, but as yet remains unquantified. However, the greater amount of hydrothermal alteration of the impact melt breccias as compared to the interior of the central uplift, suggests that the bulk of the heat must have come from the impact melt breccias.

For larger craters, however, the central uplift will likely contribute more energy to post-impact hydrothermal systems, due to increasing structural uplift and contributions from the passage of the shock wave. Indeed, the concentration of the highest temperature alteration minerals in the deeper central peak lithologies of the ~35 km diameter Manson (McCarville and Crossey 1996) and the ~80 km diameter Puchezh-Katunki (Naumov 2002) impact structures would suggest this to be the case. However, mineralization with the uplift of the ~100 km Popigai impact structure, like Haughton, is very limited in nature (Naumov 2002). It also appears that the dominant heat source for the hydrothermal system developed within the large ~250 km diameter Sudbury impact structure, Canada, was the impact melt sheet (Ames et al., Forthcoming), suggesting that more controlling factors are at work (see below).

Intensity of Impact-Induced Hydrothermal Alteration

It is notable that impact-associated hydrothermal activity at Haughton is discrete in nature and restricted to vugs and veins in the lower levels of the impact melt breccias, in the heavily faulted outer margin of the central uplift, and in the faulted crater periphery. This suggests that the impact melt breccias acted as a cap to the hydrothermal system, a view supported by the pristine, unaltered nature of impact melt and diaplectic glass clasts within the preserved impact melt breccias (Osinski et al. 2005a). In addition, the low overall intensity of alteration at Haughton is consistent with the continental setting of the impact site so that the limited supply of fluids may have been a constraining factor.

The paleogeographic setting of the Kara and Puchezh-Katunki impact structures has also been used to explain why hydrothermal alteration is more intense in these structures than at the larger Popigai structure (Naumov 2002). The former two craters formed in shallow shelf or intra-continent basins, while Popigai occurred in a continental setting (Naumov 2002). Similarly, the large ~250 km diameter Sudbury impact structure formed in a shallow subaqueous environment resulting in an extensive hydrothermal system in the crater-fill impact breccias and below the impact melt sheet (Ames et al. 1998; Ames et al. 2000, Forthcoming). Recent studies of impactites in the Yaxcopoil-1 drill hole, located in the annular trough of the Chicxulub impact structure, Mexico, suggest that alteration was facilitated and enhanced by the percolation of seawater into the underlying impactites (Ames et al. 2004; Hecht et al. 2004; Lüders and Rickers 2004; Zürcher and Kring 2004). Thus, in general, it appears that the most intensive impact-induced hydrothermal alteration takes place in craters that form in shallow continental shelf or in intra-continent shallow basins (cf. Naumov 2002).

Location of Hydrothermal Deposits within Impact Craters

Based on our studies at the Haughton impact structure and a review of the existing literature, five main locations in

an impact crater where post-impact hydrothermal deposits can form are identified.

Interior of Central Uplifts

Central uplifts are formed during the modification stage of complex impact crater formation, in structures on Earth that are >2–4 km in diameter (e.g., Melosh 1989). Widespread mineralization within central uplifts has been discovered though deep drilling (hundreds to thousands of meters) of a handful of terrestrial structures (e.g., the Manson and Puchezh-Katunki impact structures noted above). These studies reveal that the temperature of crystallization of hydrothermal minerals increases with depth as well as in towards the crater center (Naumov 2002). At Haughton, mineralization within the interior of the central uplift is minor and limited to the cementation of brecciated lithologies. This could be due to the smaller size of Haughton, for it is well known that the amount of structural uplift increases with increasing crater size (Grieve and Pilkington 1996). However, from the discussions above, it is suggested that mineralization within central uplifts in particular may be very sensitive to the paleogeographic conditions, with widespread alteration of the interior of central uplifts only occurring in craters formed in shallow shelf or intra-continent basins.

Outer Margin of Central Uplifts

Our field studies at Haughton indicate that the edge of the central uplift is characterized by a ~0.5–1.0 km wide zone of highly fractured, (sub-) vertical faults and bedding, in which hydrothermal calcite veins are abundant. The concentration of hydrothermal vein mineralization around the outer margin of central uplifts has also been documented at the ~65 km diameter Siljan impact structure, Sweden (Hode et al. 2003). As with Haughton, the outer margin of the central uplift at Siljan is intensely and complexly faulted. Mineralization occurs in the form of quartz veins in granitic rocks and calcite-fluorite-pyrite-galena veins in carbonates (Hode et al. 2003). In larger peak-ring and multi-ring impact structures, hydrothermal alteration also appears to be enhanced around the edge of central uplifts (e.g., mineralization in the Levack Gneiss Complex at the Sudbury structure, that is interpreted as the remnants of the peak ring [Ames et al. 1998, Forthcoming]).

Hydrothermal Pipe Structures and Mineralization in the Faulted Crater Periphery

Detailed field mapping carried out at Haughton has revealed the presence of over seventy pipe structures or gossans (Fig. 1b) distributed around the faulted rim of the Haughton impact structure. They have not been observed in the impact melt breccias in the crater's central area (Fig. 1b). Alteration and evidence for fluid flow along fault planes is also widespread at Haughton, indicating the importance of impact-generated fault systems in governing the location and nature of hydrothermal deposits around impact craters. This is to be expected as the locations of many mineral and ore deposits formed by sedimentary- and magmatic-related hydrothermal systems are also fault-controlled (e.g., Park and MacDiarmid 1975).

Impact Melt Rocks and Melt-Bearing Breccias

The first recognition of secondary minerals, such as clays and carbonates, at terrestrial impact structures came from studies of impact melt rocks and impact breccias (e.g., Engelhardt 1972; Grieve 1978; Floran et al. 1978). However, it was not until the work of Newsom (1980) and Allen et al. (1982), that the importance and role of hydrothermal activity as an agent of alteration was recognized. Mineralization within impact melt rocks and impact breccias is typically restricted to cavity and fracture fillings, and the minor replacement of glassy materials (e.g., Newsom 1980; Osinski et al. 2001; Naumov 2002). An exception is the Sudbury impact structure, where pervasive hydrothermal alteration of crater-fill impact breccias (Onaping Formation) resulted in a series of regionally extensive semiconformable alteration zones, above which are associated zinc-lead-copper ore deposits (Ames et al. 1998, Forthcoming).

Fieldwork carried out as part of the present study reveals that mineralization occurs preferentially towards the base and edge of the planar impact melt breccia layer at Haughton. At the Kara and Popigai structures, the mineral assemblages also indicate an increase in temperature of alteration from the top to the base of impact melt rocks (Naumov 2002). It is interesting to note that numerical modeling of hydrothermal circulation around near-surface sills, which are somewhat analogous to impact melt sheets, has shown that there is a strong tendency for the concentration of fluid flow and the production of larger convective cells at the edges of sills (Cathles et al. 1997). These studies are, therefore, consistent with the suggestion that hydrothermal systems are preferentially focused at the edge of planar impact melt sheets on Mars (Newsom 2001; Newsom et al. 2001).

Post-Impact Sedimentary Crater-Fill Deposits

Intra-crater sedimentary deposits overlying crater-fill impactites (e.g., impact melt rocks and melt-bearing breccias), have been documented at many terrestrial impact structures. If these deposits were laid while the hydrothermal system was still active, then we might expect hydrothermal alteration products to be present. This is the case at the ~24 km diameter Ries impact structure, Germany, where smectite clays and various zeolite minerals are found throughout the ~400 m thick sequence of intra-crater paleolacustrine sedimentary rocks (e.g., Stöffler et al. 1977). Importantly, the onset of sedimentation at the Ries was rapid (Riding 1979) and occurred while the impact-induced hydrothermal system was still active (e.g., Newsom et al. 1986). This is also true at the much larger Sudbury structure, where crater-fill impactites are

overlain by >2000 m of intra-crater sedimentary rocks. Detailed field and geochemical studies reveal that the lowermost, ~5–50 m thick Vermilion Formation consists of chemical sedimentary rocks, or "exhalites," that were precipitated from bicarbonate-rich fluids derived from calcite alteration in the underlying impactites (Ames 1999). There is also a metalliferous alteration halo in the overlying carbonaceous mudstones of the ~600–1000 m thick Onwatin Formation, which has been attributed to hydrothermal plume activity in the water column during deposition of intra-crater sediments (Rogers et al. 1995).

In contrast, no evidence of hydrothermal alteration products has been found within the intracrater sedimentary deposits at Haughton (Osinski and Lee 2005). This can be attributed to the fact that these sedimentary lithologies were deposited $>10^4$–10^6 years following the impact event, following a period of erosion during which the bulk of the original intracrater sedimentary deposits were removed (Osinski and Lee 2005). Thus, while post-impact sedimentary crater-fill deposits may offer the opportunity for sampling hydrothermal deposits, it is critical that the timing of deposition with respect to the impact event be ascertained.

Duration of Impact-Induced Hydrothermal Systems

One of the outstanding questions regarding hydrothermal activity at Haughton and within impact craters in general, is the duration of these systems. Calculations made for the comparably sized ~200–300 m thick suevite layer at the Ries impact structure in Germany, show that cooling from ~600 down to 100 °C took several thousand years (Pohl et al. 1977). However, since the first recognition of hydrothermal activity at Haughton (Osinski et al. 2001), it has been recognized that the crater-fill impactites are clast-rich impact melt rocks or impact melt breccias, and not clastic matrix breccias as previously thought (Osinski et al. 2005a). Thus, the heat source at Haughton may have taken substantially longer than several thousand years to cool down to ambient temperatures, thereby prolonging the lifetime of the post-impact hydrothermal system.

One of the best quantified impact-induced hydrothermal systems is that of the Sudbury impact structure (e.g., Ames et al., Forthcoming, and references therein). Geochronological data suggests that the hydrothermal system persisted for up to 2 Ma, based on purely conductive cooling of the impact melt sheet (Ames et al. 1998). However, convection was also important at Sudbury as evidenced by the pervasive alteration of the crater-fill Onaping Formation, so that "the duration of the resulting hydrothermal system may have been significantly less, from tens to hundreds of thousands of years" (Ames et al. 1998). Recent numerical modeling of the ~4 km diameter Kärdla crater, Estonia (Kirsimäe et al. 2006), suggests that hydrothermal activity can persist for a few thousand years, even in relatively small structures.

SUMMARY

Over the past few years it has been recognized that hydrothermal activity is a fundamental process during and following the modification stage of hypervelocity impact events on Earth, and probably elsewhere in the solar system. The nature and distribution of hydrothermal deposits at Haughton provides critical constraints on the plumbing within mid-size complex impact structures. Understanding the distribution of hydrothermal deposits within impact craters is important if we are to truly understand any possible economic benefits of such deposits and implications for the origin and evolution of life on Earth, and other planets including Mars.

The dominant heat source for the hydrothermal system at Haughton was the crater-fill impact melt breccias that originally filled the central area of the crater to depths of >200 m. At larger diameter craters (>30–50 km), it is likely that heat contributions from the central uplift will become more important; however, in even larger diameter impact structures >200 km (e.g., Sudbury), the crater-fill impact melt rocks appear to be the predominant heat source (Ames et al., Forthcoming). Fluid inclusion data indicate that the bulk of the mineralization at Haughton occurred at moderate temperatures of ~200–240 °C down to <60 °C. Calcite and selenite are the major alteration products, in terms of volume, with minor marcasite, quartz and goethite, and subordinate barite, celestite, fibroferrite, fluorite, and pyrite. This alteration assemblage is distinctly different to that developed at many other terrestrial impact structures (e.g., clays, zeolites, K-feldspar) (Naumov 2002), thus demonstrating the importance of host lithology in governing the type of hydrothermal alteration products that are formed.

Detailed mapping has revealed the presence of a series of hydrothermal deposits at Haughton, each associated with different structural/stratigraphic settings: (a) cavity and fracture fillings within crater-fill impact melt breccias; (b) mineralized breccias within the interior of the central uplift; (c) fracture fillings around the outer margin of the central uplift; (d) hydrothermal pipe structures and mineralization along fault surfaces in the down-faulted crater rim region. The report of hydrothermal deposits in similar settings at other, less well exposed impact structures, lends credence to our proposal that Haughton may serve as a template for locating hydrothermal deposits at other impact sites.

Acknowledgments–This study was funded in part by the Natural Sciences and Engineering Research Council of Canada (NSERC) through research grants to J.G.S. and represents a component of the Ph.D. thesis of G.R.O. Funding for G.R.O. for the 2003 field season came from the Canadian Space Agency through a post-doctoral research grant. Douglas Hall provided valuable help during SEM studies. We thank Alain Berinstain, Colleen Lenahan, Samson Ootoovak, Nesha Trenholm, and everyone involved in the NASA

Haughton-Mars Project for their assistance during the HMP 1999–2003 field seasons. Doreen Ames and Horton Newsom are sincerely thanked for their constructive and helpful reviews. This is contribution HMP-SCI 2004-002. PASSC publication #39.

Editorial Handling—Dr. Elisabetta Pierazzo

REFERENCES

Allen C. C., Gooding J., and Keil K. 1982. Hydrothermally altered impact melt rock and breccia: Contributions to the soil of Mars. *Journal of Geophysical Research* 87:10,083–10,101.

Ames D. E., Watkinson D. H., and Parrish R. R. 1998. Dating of a regional hydrothermal system induced by the 1850 Ma Sudbury impact event. *Geology* 26:447–450.

Ames D. E. 1999. Geology and regional hydrothermal alteration of the crater-fill Onaping Formation: Association with Zn-Pb-Cu mineralization, Sudbury Structure, Canada. Ph.D. thesis, Carleton University, Ottawa, Ontario, Canada.

Ames D. E., Gibson H. L., and Watkinson D. H. 2000. Controls on major impact-induced hydrothermal system, Sudbury Structure, Canada (abstract #1873). 31st Lunar and Planetary Science Conference. CD-ROM.

Ames D. E., Golightly J. P., Lightfoot P. C., and Gibson H. L. 2002. Vitric compositions in the Onaping Formation and their relationship to the Sudbury Igneous Complex, Sudbury Structure. *Economic Geology* 97:1541–1562.

Ames D. E., Kjarsgaard I. M., Pope K. O., Dressler B. O., and Pilkington M. 2004. Secondary alteration of the impactite and mineralization in the basal Tertiary sequence, Yaxcopoil-1, Chicxulub impact crater, Mexico. *Meteoritics & Planetary Science* 39:1145–1167.

Ames D. E., Jonasson J. R., Gibson H. L., and Pope K. O. Forthcoming. Impact-generated hydrothermal system: Constraints from the large Paleoproterozic Sudbury crater, Canada. In *Biological processes associated with impact events*, edited by Cockell C. S., Gilmour I., and Koeberl C. Berlin: Springer-Verlag. 376 p.

Cathles L. M., Erendi A. H. J., and Barrie T. 1997. How long can a hydrothermal system be sustained by a single intrusive event? *Economic Geology* 92:766–771.

Cockell C. S. and Lee. P. 2002. The biology of impact craters: A review. *Biological Reviews* 77:279–310.

Daubar I. J. and Kring D. A. 2001. Impact-induced hydrothermal systems: Heat sources and lifetimes (abstract #1727). 32nd Lunar and Planetary Science Conference. CD-ROM.

Engelhardt W. V. 1972. Shock produced rock glasses from the Ries crater. *Contributions to Mineralogy and Petrology* 36:265–292.

Farmer J. D. 2000. Hydrothermal systems: Doorways to early biosphere evolution. *GSA Today* 10:7:1–9.

Floran R. J., Grieve R. A. F., Phinney W. C., Warner J. L., Simonds C. H., Blanchard D. P., and Dence M. R. 1978. Manicouagan impact melt, Quebec. I: Stratigraphy, petrology, and chemistry. *Journal of Geophysical Research* 83:2737–2759.

Goldhaber M. B. and Stanton M. R. 1987. Experimental formation of marcasite at 150–200 °C: Implications for carbonate-hosted Pb/Zn deposits (abstract). Geological Society of America Annual Meeting. p. 678.

Graup G. 1999. Carbonate-silicate liquid immiscibility upon impact melting: Ries Crater, Germany. *Meteoritics & Planetary Science* 34:425–438.

Grieve R. A. F. 1978. The melt rocks at the Brent Crater, Ontario. Proceedings, 9th Lunar and Planetary Science Conference. pp. 2579–2608.

Grieve R. A. F. and Masaitis V. L. 1994. The economic potential of terrestrial impact craters. *International Geology Reviews* 36: 105–151.

Grieve R. A. F. and Pilkington M. 1996. The signature of terrestrial impacts. *Australian Geology and Geophysics Journal* 16:399–420.

Grieve R. A. F., Dence M. R., and Robertson P. B. 1977. Cratering processes: As interpreted from the occurrence of impact melts. In *Impact and explosion cratering*, edited by Roddy D. J., Pepin R. O., and Merrill R. B. New York: Pergamon Press. pp. 791–814.

Hagerty J. J. and Newsom H. E. 2003. Hydrothermal alteration at the Lonar Lake impact structure, India: Implications for impact cratering on Mars. *Meteoritics & Planetary Science* 38:365–382.

Hecht L., Wittmann A., Schmitt R. T., and Stöffler D. 2004. Composition of impact melt particles and the effects of post-impact alteration in suevitic rocks at the Yaxcopoil-1 drill core, Chicxulub crater, Mexico. *Meteoritics & Planetary Science* 39: 1169–1186.

Hickey L. J., Johnson K. R., and Dawson M. R. 1988. The stratigraphy, sedimentology, and fossils of the Haughton Formation: A post-impact crater fill. *Meteoritics* 23:221–231.

Hode T., von Dalwigk I., and Broman C. 2003. A hydrothermal system associated with the Siljan impact structure, Sweden—Implications for the search for fossil life on Mars. *Astrobiology* 3:271–289.

Kieffer S. W. and Simonds C. H. 1980. The role of volatiles and lithology in the impact cratering process. *Reviews of Geophysics and Space Physics* 18:143–181.

Kirsimäe K., Jõeleht A., Plado J., Versh E., and Ainsaar L. 2006. Development of ecological niches in impact-induced hydrothermal systems—The case of the Kärdla Crater (abstract). In *Biological processes associated with impact events*, edited by Cockell C., Koeberl C., and Gilmour I. Berlin: Springer. 376 p.

Kring D. A. 2000. Impact events and their effect on the origin, evolution, and distribution of life. *GSA Today* 10:8:1–7.

Lüders V. and Rickers K. 2004. Fluid inclusion evidence for impact-related hydrothermal fluid and hydrocarbon migration in Cretaceous sediments of the ICDP-Chicxulub drill core Yax-1. *Meteoritics & Planetary Science* 39:1187–1197.

McCarville P. and Crossey L. J. 1996. Post-impact hydrothermal alteration of the Manson impact structure. In *The Manson impact structure, Iowa: Anatomy of an impact crater.* Special Paper #302, edited by Koeberl C. and Anderson R. R. Boulder, Colorado: Geological Society of America. pp. 347–376.

Melosh H. J. 1989. *Impact cratering: A geologic process*. New York: Oxford University Press. 245 p.

Metzler A., Ostertag R., Redeker H. J., Stöffler D. 1988. Composition of the crystalline basement and shock metamorphism of crystalline and sedimentary target rocks at the Haughton impact crater. *Meteoritics* 23:197–207.

Moore J. N., Adams M. C., and Anderson A. J. 2000. The fluid inclusion and mineralogic record of the transition from liquid- to vapor-dominated conditions in the Geysers geothermal system, California. *Economic Geology* 95:1719–1737.

Moore J. N., Allis R., Renner J. L., Mildenhall D., and McCulloch J. 2002. Petrologic evidence for boiling to dryness in the Karaha-Telaga Bodas geothermal system, Indonesia. Proceedings, 27th Workshop on Geothermal Reservoir Engineering. pp. 98–108.

Murowchick J. B. and Barnes H. L. 1986. Marcasite precipitation from hydrothermal solutions. *Geochimica et Cosmochimica Acta* 50:2615–2629.

Naumov M. V. 2002. Impact-generated hydrothermal systems: Data

from Popigai, Kara, and Puchezh-Katunki impact structures. In *Impacts in Precambrian shields*, edited by Plado J. and Pesonen L. J. Berlin: Springer-Verlag. pp. 117–171.

Newsom H. E. 1980. Hydrothermal alteration of impact melt sheets with implications for Mars. *Icarus* 44:207–216.

Newsom H. E. 2001. Central remnant craters on Mars—Localization of hydrothermal alteration at the edge of crater floors? (abstract #1402). 32nd Lunar and Planetary Science Conference. CD-ROM.

Newsom H. E., Graup G., Sewards T., and Keil K. 1986. Fluidization and hydrothermal alteration of the suevite deposit in the Ries Crater, West Germany, and implications for Mars. *Journal of Geophysical Research* 91:239–251.

Newsom H. E., Hagerty J. J., and Thorsos I. E. 2001. Location and sampling of aqueous and hydrothermal deposits in martian impact craters. *Astrobiology* 1:71–88.

Nicholson K. 1993. *Geothermal fluids: Chemistry and exploration techniques*. Berlin: Springer-Verlag. 263 p.

Osinski G. R. 2003. Impact glasses in fallout suevites from the Ries impact structure, Germany: An analytical SEM study. *Meteoritics & Planetary Science* 38:1641–1667.

Osinski G. R. and Lee P. 2005. Intra-crater sedimentary deposits of the Haughton impact structure, Devon Island, Canadian High Arctic. *Meteoritics & Planetary Science* 40. This issue.

Osinski G. R. and Spray J. G. 2001. Impact-generated carbonate melts: Evidence from the Haughton structure, Canada. *Earth and Planetary Science Letters* 194:17–29.

Osinski G. R. and Spray J. G. 2003. Evidence for the shock melting of sulfates from the Haughton impact structure, Arctic Canada. *Earth and Planetary Science Letters* 215:357–270.

Osinski G. R. and Spray J. G. 2005. Tectonics of complex crater formation as revealed by the Haughton impact structure, Devon Island, Canadian High Arctic. *Meteoritics & Planetary Science* 40. This issue.

Osinski G. R., Spray J. G., and Lee P. 2001. Impact-induced hydrothermal activity within the Haughton impact structure, Arctic Canada: Generation of a transient, warm, wet oasis. *Meteoritics & Planetary Science* 36:731–745.

Osinski G. R., Grieve R. A. F., and Spray J. G. 2004. The nature of the groundmass of the Ries impact structure, Germany, and constraints on its origin. *Meteoritics & Planetary Science* 39: 1655–1684.

Osinski G. R., Spray J. G., and Lee P. 2005a. Impactites of the Haughton impact structure, Devon Island, Canadian High Arctic. *Meteoritics & Planetary Science* 40. This issue.

Osinski G. R., Lee P., Spray J. G., Parnell J., Lim D. S. S., Bunch T. E., Cockell C. S., and Glass B. 2005b. Geological overview and cratering model of the Haughton impact structure, Devon Island, Canadian High Arctic. *Meteoritics & Planetary Science* 40. This issue.

Park C. F. and MacDiarmid R. A. 1975. *Ore deposits*. San Francisco: W. H. Freeman and Company. 529 p.

Parnell J., Osinski G. R., Lee P., Baron M., Pearson M. J., and Feely M. 2003. Hydrocarbons in the Haughton impact structure, Devon Island, Nunavut, Canada (abstract #1118). 34th Lunar and Planetary Science Conference. CD-ROM.

Parnell J., Lee P., Osinski G. R., and Cockell C. S. 2005. Application of organic geochemistry to detect signatures of organic matter in the Haughton impact structure. *Meteoritics & Planetary Science* 40. This issue.

Pirajno F. 1992. *Hydrothermal mineral deposits: Principles and fundamental concepts for the exploration geologist*. Berlin: Springer-Verlag. 709 p.

Pierazzo E., Artemieva N. A., and Ivanov B. 2005. Starting conditions for hydrothermal systems underneath martian craters: Hydrocode modeling. In *Large meteorite impacts III*. Special Paper #384, edited by Kenkmann T., Hörz F., and Deutsch A. Boulder, Colorado: Geological Society of America.

Pohl J., Stöffler D., Gall H., and Ernstson K. 1977. The Ries impact crater. In *Impact and explosion cratering*, edited by Roddy D. J., Pepin R. O., and Merrill R. B. New York: Pergamon Press. pp. 343–404.

Rathbun J. A. and Squyres S. W. 2002. Hydrothermal systems associated with martian impact craters. *Icarus* 157:362–372.

Riding R. 1979. Origin and diagenesis of lacustrine algal bioherms at the margin of the Ries Crater, upper Miocene, southern Germany. *Sedimentology* 26:645–680.

Roedder E. 1981. Origin of fluid inclusions and changes that occur after trapping. In *Short course in fluid inclusions. Applications to Petrology*, edited by Hollister L. S. and Crawford M. L. Calgary: Mineralogical Association of Canada. pp. 107–137.

Rogers D. F., Gibson H. L., Whitehead R., Checetto J., and Jonasson E. R. 1995. Structure and metal enrichment in the hanging wall carbonaceous argillites of the Paleoproterozoic Vermilion and Errington Zn-Cu-Pb massive sulfide deposits, Sudbury, Canada (abstract). Proceedings, Geological Association of Canada–Mineralogical Association of Canada. 20:A90.

Schoonen M. A. A. and Barnes H. L. 1991a. Reactions forming pyrite and marcasite from solution: I. Nucleation of FeS_2 below 100 °C. *Geochimica et Cosmochimica Acta* 55:1495–1504.

Schoonen M. A. A. and Barnes H. L. 1991b. Reactions forming pyrite and marcasite from solution: II. Via FeS precursors below 100 °C. *Geochimica et Cosmochimica Acta* 55:1505–1514.

Schoonen M. A. A. and Barnes H. L. 1991c. Mechanisms of pyrite and marcasite formation from solution: III. Hydrothermal processes. *Geochimica et Cosmochimica Acta* 55:3491–3504.

Scott D. and Hajnal Z. 1988. Seismic signature of the Haughton structure. *Meteoritics* 23:239–247.

Sherlock S. C., Kelley S. P., Parnell J., Green P., Lee P., Osinski G. R., and Cockell C. S. 2005. Re-evaluating the age of the Haughton impact event. *Meteoritics & Planetary Science* 40. This issue.

Shepherd T. J., Rankin A. H., and Alderton D. H. M. 1985. *A practical guide to fluid inclusions*. Glasgow: Blackie. 239 p.

Shock E. L. 1996. Hydrothermal systems as environments for the emergence of life. In *Evolution of hydrothermal ecosystems on Earth (and Mars?)*, edited by Bock G. R. and Goode J. A. Chichester: John Wiley & Sons Ltd. pp. 40–82.

Stöffler D., Ewald U., Ostertag R., and Reimold W. U. 1977. Research drilling Nördlingen 1973 (Ries): Composition and texture of polymict impact breccias. *Geologica Bavarica* 75: 163–189.

Thorsteinsson R. and Mayr U. 1987. *The sedimentary rocks of Devon Island, Canadian Arctic Archipelago*. Geological Survey of Canada Memoir #411. Ottawa: Geological Survey of Canada. 182 p.

White D. E., Muffler L. J. P., and Truesdell A. H. 1971. Vapor-dominated hydrothermal systems compared with hot water systems. *Economic Geology* 66:75–97.

Zürcher L. and Kring D. A. 2004. Hydrothermal alteration in the core of the Yaxcopoil-1 borehole, Chicxulub impact structure, Mexico. *Meteoritics & Planetary Science* 39:1199–1221.